JOURNAL OF GEOPHYSICAL RESEARCH, VOL. 103, NO. A8, PAGES 17,223–17,233, AUGUST 1, 1998

Electron beams and radio waves of solar Type III bursts

George A. Dulk,[1] Yolande Leblanc,[1] Peter A. Robinson,[2] Jean-Louis Bougeret,[1] and Robert P. Lin[3]

Abstract. Using the radio wave and energetic particle experiments on the Wind spacecraft, we examine how the radio flux density of interplanetary type III bursts depends on the flux and energy of the energetic electrons. We derive the relationship between them, first by giving detailed radio and electron characteristics of one type III burst, and then using the results of similar analyses of 10 bursts. The times of commencement of the radio waves from decametric to kilometric wavelengths, in relation to the onset time of Langmuir waves, demonstrate forcibly that the initial type III radiation is at the fundamental and not the harmonic. Near and after the time of peak flux density the radiation could be either at the fundamental or the harmonic. In our theoretical analysis we examine this point, i.e., how the emissivity of the fundamental and harmonic at the time of peak flux density depends on the beam properties. The data of the 10 events are in good accord ($r_c \approx 0.9$) with the theoretical relation for fundamental emission, but in disaccord with the theoretical relation for harmonic radiation. For the 10 bursts we find poor correlation between the radio flux density and the electron flux $N(E_{||})$ at the energy $E_{||}$ estimated to be that of the two-stream instability. However there is excellent correlation when $N(E_{||})$ is weighted by $E_{||}$ to a high power. From the best fit, we find $r_c \approx 0.96$ when $N(E_{||})$ is replaced by $E_{||}^{3.98} N(E_{||})$. Finally, we infer the efficiency of energy conversion from the kinetic energy of the electron beam to fundamental emission, and examine the attenuation of the peak emission within the source.

1. Introduction

It is well established that solar type III bursts are generated by beams of energetic electrons ejected from the Sun that travel outward along open magnetic field lines through the corona and the interplanetary space. Along their path they generate high levels of Langmuir waves at the plasma frequency f_p, and some of the energy of the Langmuir waves is converted into electromagnetic radiation either at the fundamental, $f = f_p$, the second harmonic, $f = 2f_p$, or both.

Type III bursts have been observed intensively with ground-based and space-based instruments; in situ electrons and Langmuir waves have been directly associated with type III emission [*Gurnett and Anderson,* 1976; *Lin et al.,* 1981]. In particular it was shown that the presence of Langmuir waves observed in situ coincided with the bump on tail in the electron parallel velocity distribution [*Lin et al.,* 1981, 1996].

[1]CNRS-URA 264, Department de Recherche Spatiale, Observatoire de Paris, Meudon, France.
[2]School of Physics, University of Sydney, Australia.
[3]Space Sciences Laboratory, University of California, Berkeley.

Paper number 97JA03061.
0148-0227/98/97JA-03061$09.00

The most recent study [*Ergun et al.,* 1997; see also *Lin,* 1997] which used instruments on the Wind spacecraft, reports detailed observations of the event of April 2, 1995, when four electron events coincided with solar type III bursts. Accompanying two of the bursts were Langmuir waves that commenced with the arrival of ~ 10 keV electrons. There were very few occurrences of unstable distributions (reduced distributions: $f(v_{||})$ vs.$v_{||}$ which showed a positive slope with 96-s-averaged data), with the marginally stable or slightly unstable distributions being observed at times when Langmuir wave spikes were occurring.

A theoretical picture of type III emission was first advanced by *Ginzburg and Zheleznyakov* [1958], and, with some modifications, the core of this picture is still current today: Langmuir waves are generated by a bump-on-tail instability of the electron beam. Growth of Langmuir waves then tends to relax the beam toward marginal stability by quasilinearly flattening its velocity distribution. Nonlinear wave-wave interactions involving the Langmuir waves then lead to fundamental and harmonic radio emission. The recently developed stochastic-growth theory (SGT) of type III radio bursts has shown that propagation of the beam with fluctuations about marginal stability can account for the clumpiness of the observed Langmuir waves [*Robinson,* 1992; *Robinson et al.,* 1992, 1993a], the production

of associated ion-sound waves [*Robinson et al.,* 1993b; *Cairns and Robinson,* 1995], and the observed radio emissivities [*Robinson and Cairns,* 1993; *Robinson et al.,* 1994; *Robinson and Cairns,* 1994; *Willes et al.,* 1996; *Willes and Robinson,* 1997]. Recently, *Robinson* [1996] showed how SGT can be used to estimate the volume radio emissivity more directly from the electron flux and the conversion efficiency from electron kinetic energy to waves.

The purpose of this paper is to determine how the characteristics of the electron beams are related to the characteristics of the associated type III bursts and to determine whether this relationship is consistent with the predictions of SGT. To our knowledge there has not been a study of the correlation between the flux of the electrons and the radio flux density. This information is important for determining the efficiency of the emission process.

Following, in Section 2 we briefly describe the observational techniques, in Section 3 we present electron and radio data of a sample event. In Section 4, for the ten events observed, we compile data on radio flux densities, and energies and fluxes of the energetic electrons. In Sections 5 and 6 we develop the theory and show that the correlations between the data are consistent with those predicted by SGT on the assumption that the peak radio flux is due to fundamental emission. In Section 7 we summarize and give concluding remarks.

2. Electron and Radio Observations

The Wind spacecraft is always near Earth, in the ecliptic plane, near 1 AU. Radio waves are observed from remote locations, from near the Sun to more than 1 AU, and from bursts that originate anywhere, even directly behind the Sun. Here we concentrate on bursts for which Wind was within the path of the electron streams, where the impulsive electron fluxes were observed with the three-dimensional (3-D) plasma instrument; the associated Langmuir waves and solar type III bursts were observed with the Radio and Plasma Wave Investigation (WAVES) instrument. Combining the data from the two experiments allows the study of the characteristics of events observed simultaneously.

Impulsive electron events are observed with the 3-D Plasma and Energetic Particle experiment [*Lin et al.,* 1995], and for the first time, impulsive solar electrons are detected in an extended range from 300 down to 0.4 keV. Compared with previous experiments, this one has better angular resolution and full coverage of velocity space.

Radio bursts are observed mainly with the WAVES experiment [*Bougeret et al.,* 1995]. It consists of long dipole antennas in the spin plane and short antennas along the spin axis, feeding into three receivers covering the range from 4 kHz to 13.8 MHz. Complemented by 25 to 75 MHz data from the Nançay array [*Boischot et al.,* 1980] for one burst, this is the first time that type III bursts are observed in the very large frequency range from 75 MHz to a few kHz, which allows a measure of the flux density spectrum of emissions occurring from about 1.4 solar radii to 1 AU or more. In addition, time profiles over this large range of frequency give accurate information on how groups of bursts at coronal heights merge together to form one interplanetary burst, and on the disappearance and/or emergence of burst components at intermediate or low frequencies. The composite then gives rise to a very broad low frequency burst that sometimes descends just to the plasma frequency.

Here we use the traces of onset times of the radio radiation extrapolated to the time of the Langmuir waves to derive the velocity $v_{\|}$ of the exciting electrons that travel along the magnetic field, and to determine the emission mode, fundamental (F) or harmonic (H). From the energy spectra of the electrons we estimate the critical energy where a positive slope in the reduced distribution function exists at the time of the commencement of the Langmuir waves. This critical energy is compared with the parallel energy $E_{\|}$ derived from the radio waves and the average pitch angle of the electrons is derived. The electron flux at the critical energy is then compared with the flux density of the radio waves, and the relationship between them is derived.

We concentrate on the first year of Wind observations, during which there were 14 electron events suitable for analysis. Of these, four were eliminated because the electron spectra did not extend to sufficiently low energies. Thus we are left with 10 events where we could compare the electron and radio observations.

3. Electrons and Radio Waves of a Sample Burst

Here we give the detailed characteristics of the electron and radio observations of one of the ten bursts of the study. We choose to illustrate the burst of April 2, 1995, 1100 UT, which has most of the same features as the others but is one of the most intense in terms of radio waves and electron fluxes. In part we choose it because detailed analysis of the electron properties is contained in the papers of *Ergun et al.* [1997] and *Lin* [1997], including a plot of the 3-D distribution function and a series of reduced distributions, $f(v_{\|})$ versus $v_{\|}$. The present study clarifies the relationship between the radio waves and the fluxes of energetic electrons.

3.1. Properties of the Electrons

Figure 1 shows time histories of the electron flux at 12 energies recorded by the 3-D plasma experiment on Wind. The vertical dashed lines enclose the times that Langmuir waves were present. Increases of electron flux are visible at all energies down to 1.3 keV, whose maximum was well after the end of the Langmuir waves.

At the first occurrence of Langmuir waves, 1146 UT, electrons of $E = 19$ keV had commenced about 10 min earlier and those of $E = 13$ keV were starting, while at higher energies the fluxes had already peaked or were about to do so. From this we estimate which electrons generate the Langmuir waves, i.e., the energy at which there was a positive slope in the reduced distribution, we find 13 – 20 keV. This estimate can be compared

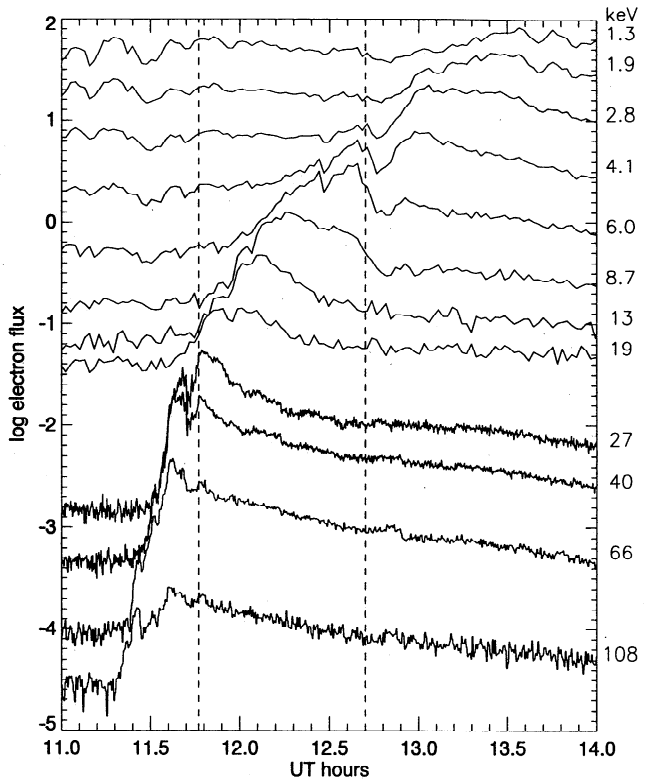

Figure 1. Energetic electron fluxes at 12 energies as recorded by the 3-D plasma experiment on Wind. The vertical dashed lines show the times of beginning and end of Langmuir waves. The units are $(\text{cm}^2\ \text{s ster eV})^{-1}$.

with the detailed study of this event by *Ergun et al.* [1997], who found a marginally stable or slightly unstable reduced distribution in 96 s-averaged data at times when Langmuir waves were recorded (reduced distributions on shorter time scales are not available; these might well have shown a higher degree of instability). Ergun et al. found that the positive slope occurred where the beam velocity was $v_{\|} \approx 6 \times 10^4$ km s^{-1} ($E_{\|} \approx 10$ keV). Assuming a typical pitch angle of 40° (see below) the total energy was $E \approx 17$ keV.

Figure 2 shows some derived properties of the electrons. Figure 2a shows the times of commencement and of maximum electron flux as a function of the electron energy, with the dotted lines showing the start and end times of the Langmuir waves. For example, at the initial time of Langmuir waves, ≈11 keV electrons were just starting to arrive, and ≈27 keV electrons were attaining their maximum flux. At the time of the last Langmuir waves, ≈2.5 keV electrons were starting to arrive and ≈5 keV electrons were attaining their maximum flux.

Figure 2b shows the electron flux as a function of energy, measured at the time of the maximum of flux. A straight line gives a good fit over most of the range of energies, indicating that $N(E)$ versus E is approximately a power law.

The average pitch angle $\alpha_e(E)$ of the initial electrons at each energy can be derived from their time of arrival at Wind and the time of acceleration at the Sun. We take the distance along the spiral to be 1.15 AU and the acceleration time to be 1056 UT (from the high-frequency radio waves, corrected for light travel time). Then knowing the arrival time at each energy we calculate $v_{\|}$ and $E_{\|}$, and then the pitch angle $\alpha_e(E) = \arccos(E_{\|}/E)^{1/2}$.

Figure 2c shows how this average pitch angle varies with energy, decreasing from about 50° at 100 keV to about 10° at 1.5 keV. This is a typical characteristic, as pointed out by *Lin et al.* [1996], who noted that the large divergence of the magnetic field outward from the Sun should collimate all electrons to very small pitch angles, and therefore that the large pitch angles observed at high energies probably result from pitch angle scattering along the path.

3.2 Properties of the Radio Waves

Figure 3 shows the dynamic spectrum of the type III burst over a large and unprecedentedly complete spectral range. Figure 3c, from the decametric array at Nançay, France, shows the relevant group of type III bursts as they traversed the inner corona from about

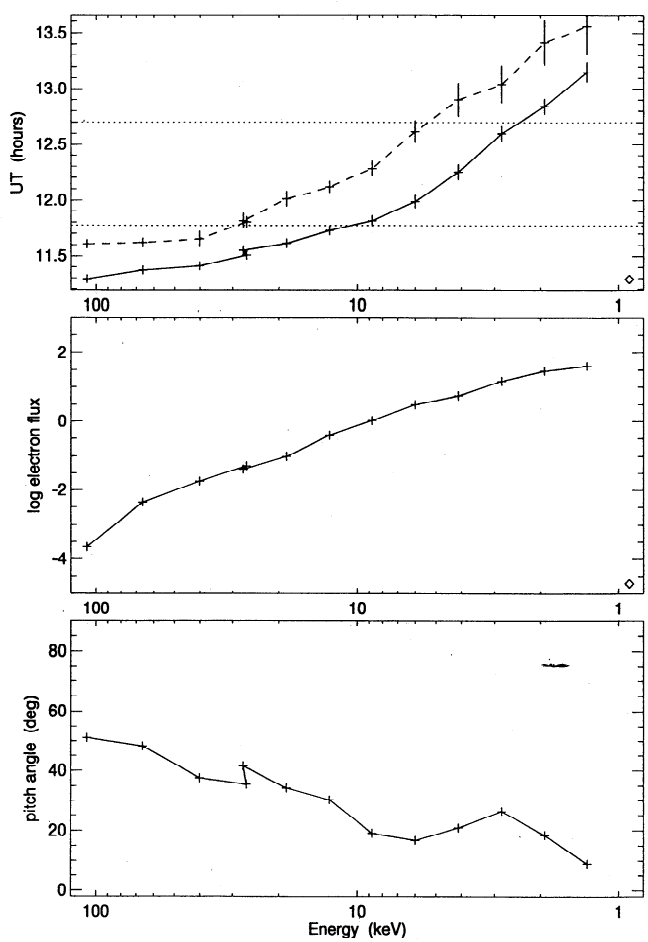

Figure 2. (top): Times of commencement (solid line) and of peak flux (dashed line) of electrons at various energies. The dotted lines show the times of beginning and end of Langmuir waves. (middle): Peak electron flux at each energy in units of $(\text{cm}^2\ \text{s ster eV})^{-1}$. (bottom): Average pitch angle from the Sun to Wind of electrons of each energy.

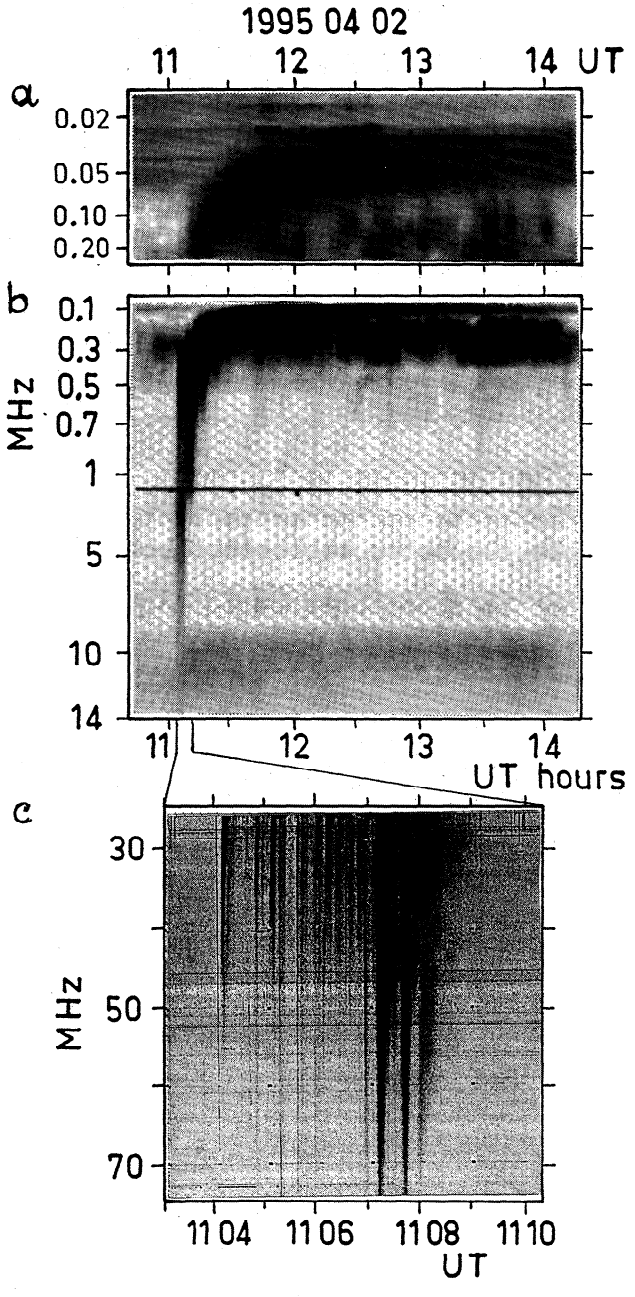

Figure 3. Dynamic spectrum of the type III burst group of April 2, 1995, 1100 UT, as recorded by (a) the thermal noise receiver of Wind, (b) two radio receivers of Wind, and (c) the decametric array at Nançay, France. The spectral coverage is unprecedented, with a gap only from 13.8 to 25 MHz.

1.4 R_o (75 MHz) to about 2.5 R_o (25 MHz). About 20 bursts are identifiable between 1104 and 1108 UT, with the strongest two occurring after 1107 UT. Close examination shows that there is *F/H* structure in some of the bursts, a strong *F* component followed by a weaker H component. From analysis not shown here we find that the degree of circular polarization is higher for the fundamental than for the harmonic, which is typical of *F/H* pairs [e.g., *Dulk and Suzuki,* 1980]. The intense fundamentals are 25 to 50% LH polarized, while the weaker harmonics are $\lesssim$10% polarized.

Figure 3b shows the development of the burst from 13.8 MHz to 20 kHz, ≈ 3 R_o to 1 AU, as recorded by the WAVES experiment on Wind. The time scale is greatly different because the burst duration increases rapidly with decreasing frequency. Between about 0.1 and 0.3 MHz the spectrum is contaminated by intense auroral kilometric radiation (AKR).

Figure 3a shows the lowest frequencies in more detail. The sporadic, intense, narrow-band radiation at 0.025 MHz that lasts about an hour is due to Langmuir wave spikes at the local plasma frequency, i.e., $f_{pW} = 25$ kHz. The onset time of the radio waves with decreasing frequency leads to the onset time of the Langmuir waves.

To see this in more detail, Figure 4 shows the time history of the burst at 14 frequencies as recorded on Wind. The highest frequency, 13.8 MHz, arises in the corona at about 3 R_o, while the lowest frequency, 28 kHz arises in the solar wind at almost 1 AU. At the higher frequencies, above a few MHz, the structure is much the same as in the decametric spectrum of Figure 3, with weak bursts at first, then the stronger ones. Detailed views of five traces are boxed in the lower right, where the time scale is enlarged by a factor of 10. The sequence shows that the early bursts build up their intensity relative to the later ones, while fine-scale features broaden. At 196 kHz (emitted near 0.1 AU in density models used and justified later) and below, all bursts of the group merge into one, smooth burst. (At frequencies between 80 and 388 kHz the erratic variations are due to contamination by AKR.)

The thermal noise receiver on Wind (see Figure 3a) records the quasi-thermal plasma line; it shows that the local plasma frequency was $f_{pW} = 25$ kHz, and that Langmuir wave spikes were present between 1146 and 1242 UT; these two times are shown in Figure 4 by the vertical dashed lines. At 28 kHz the radio flux density begins to rise just before the Langmuir waves commence; the three short peaks are due to Langmuir spikes leaking from 25-kHz into the 28-kHz channel.

We have measured the times of commencement and of the peak of the burst at each frequency, the radio flux density of the background, and that of burst maximum. Figure 5 shows these times and the peak flux density after background subtraction. On Figure 5a the right-hand ordinate shows the frequencies on a scale that is proportional to f^{-1}. The left-hand scale is derived assuming that $n_e \propto R^{-2}$, so that $R \propto f_p^{-1}$. The constant of proportionality is fixed by knowing that $f_p(1\text{ AU}) = f_{pW} = 25$ kHz. The interval where Langmuir waves were recorded at 25 kHz (1 AU) is marked by the open squares. The solid line is the trace of electrons travelling at constant speed along an Archimedean spiral of length 1.15 AU from the Sun to Wind, starting at the acceleration time at the Sun as given by the type III burst at high frequencies, and arriving at the time of the Langmuir wave commencement; the corresponding electron speed is $v_{\|} = 0.19$ c. (Here we have corrected

for light-travel time, 8 min for the highest frequencies originating in the corona, and proportionally less for lower frequencies arising farther from the Sun.)

The stars on Figure 5a that denote burst starting times at various radio frequencies lie closely along the solid line, and with very little extrapolation they lead to the start of the Langmuir waves. This is direct evidence that the initial radiation of the type III is at the fundamental; e.g., Langmuir waves at 25 kHz generate 25 kHz radiation.

The dashed line on Figure 5a indicates the trace of burst starting times at various frequencies if the radiation were at the harmonic. It is at twice the frequency of the solid line, leading from the flare to $2f_{pW}$ at the start of the Langmuir waves. It denotes the earliest time that harmonic radiation could begin; e.g., starting at 11.75^h UT, Langmuir waves at 1 AU (where $f_p = f_{pW} = 25$ kHz) could generate harmonic radiation at 50 kHz. At frequencies below 50 kHz, harmonic radiation must originate at distances beyond 1 AU and must travel upwind toward the spacecraft; e.g., the source of 28 kHz H radiation must lie nearly at 2 AU.

The triangles on Figure 5a denote the times of maximum radio flux density at each frequency. The triangles do not converge to the burst start time at the highest frequencies because they refer to the strongest burst, which occurred late in the burst group. The triangles follow the same slope as the dashed line that represents possible beginning of H radiation, and lie after it. Therefore the radiation at the time of radio flux maximum could be fundamental, harmonic, or a combination of the two. In earlier studies and in the other nine events of this study, the times of flux maxima were generally near the earliest time that harmonic radiation could begin (dashed lines), sometimes slightly before and sometimes slightly after. This suggests that if there is a gradual changeover from fundamental radi-

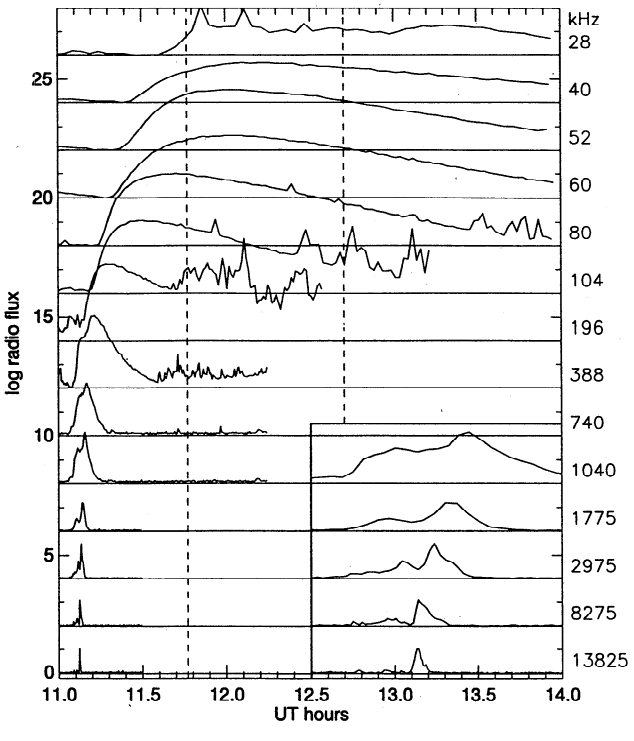

Figure 4. Flux density versus time for 14 of the frequencies recorded by the WAVES experiment on Wind. Each unit of the ordinate represents a radio flux density increase of a factor of 10 above background, and subsequent panels are offset by 2 in the log. In the box at bottom right are the same traces as at the left but with a 10 times expanded timescale. The vertical, dashed lines show the start and end times of Langmuir wave spikes.

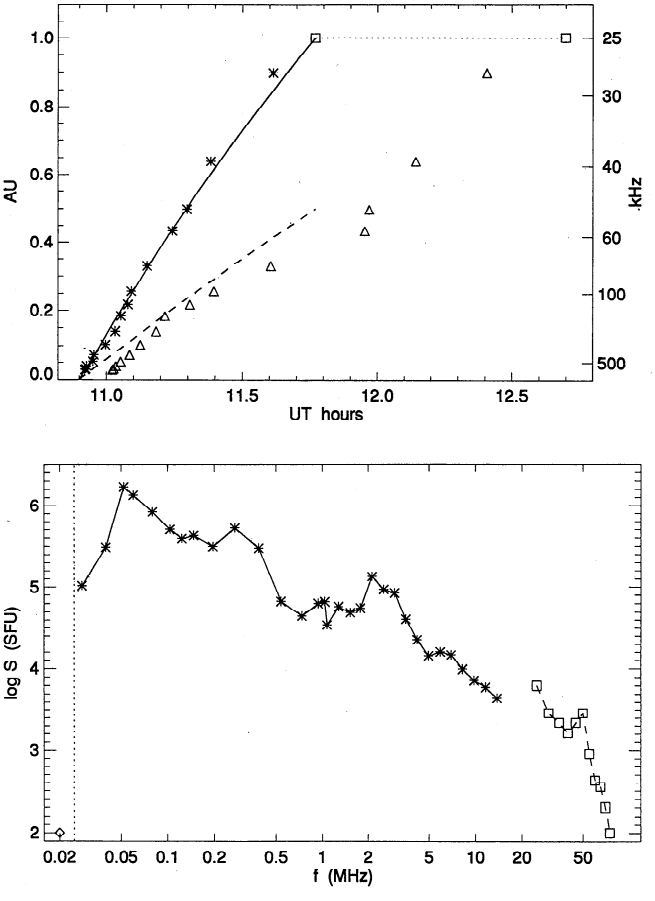

Figure 5. (top): Start times (stars) and times of peak flux density (triangles) of radio waves at different frequencies (right scale) that are emitted at different distances from the Sun (left scale). A correction for light travel time has been included. The squares connected by the dotted line show the interval of Langmuir waves. The solid line is the trace of electrons of $v_{\|} = 0.19$ c that emit radiation at the fundamental as they travel along an Archimedean spiral from the Sun to Wind, starting at the acceleration time as given by the type III burst at high frequencies and arriving at Wind at the time of the commencement of Langmuir waves. The dashed line would be the trace of the same electrons if they emitted only harmonic radiation. (bottom): Spectrum of the radio burst as measured at the time of peak flux density at each frequency. The stars are measurements by the WAVES experiment on Wind and the squares are measurements by the decametric array at Nançay, France. The dotted line denotes the plasma frequency at Wind: 25 kHz.

Table 1. Derived Parameters for the 10 Type III/Electron Events

Event	Date	Universal Time	L Waves	$v_\parallel$	$E_\parallel$ keV	E_1 keV	⟨Pitch Angle⟩	log S_{radio} (at $2f_p$)	$N(E_1)$ (at 1.5 E_0)
1	Dec. 27, 1994	1040	y	0.14 c	5.0	14.5	54°	5.5	0.10
2	Jan. 23, 1995	1550	n	0.09 c	2.1	4.5	47°	4.1	0.10
3	Feb. 2, 1995	0315	n	0.10 c	2.6	7.5	54°	4.2	0.08
4	Apr. 4, 1995	0440	n	0.15 c	5.8	16.5	53°	5.5	0.02
5	Apr. 4, 1995	0830	n	0.17 c	7.4	15.0	45°	5.0	0.03
6	Apr. 4, 1995	1105	y	0.19 c	9.2	16.5	34°	6.2	0.16
7	Apr. 4, 1995	1420	y	0.18 c	8.3	19.0	49°	6.3	0.07
8	June 30, 1995	0405	y	0.10 c	2.6	6.0	49°	4.1	0.06
9	Oct. 10, 1995	1025	y	0.10 c	2.6	4.5	40°	5.1	5.0
10	Oct. 20, 1995	0550	y	0.19 c	9.2	17.0	43°	6.7	2.0

ation being dominant to harmonic being dominant, it occurs near or after the flux maximum.

Figure 5b shows the spectrum of the radio flux density (at the time of maximum at each frequency) over an unprecedentedly large frequency range, with only a small gap from 14 to 25 MHz. In the Wind measurements from 28 kHz to 14 MHz the flux density does not have a constant value but varies between about 10^5 and 2×10^6 SFU, with the maximum occurring at about twice the plasma frequency. Above 1 MHz the calibration of the receiver is still being examined, but the values given should be accurate to a factor of about 2. Above about 10 MHz there is the usual rapid decrease in flux density toward metric wavelengths [see also *Steinberg et al.*, 1984].

4. Electron and Radio Data for the 10 Events

For each of the 10 electron events for which we have adequate data we performed the same detailed analysis as for the sample event just described. Here we use the results of those analyses to derive the relationship between the flux and energy of energetic electrons and the flux density of the radio waves.

As explained above, the energy of electrons where there is a positive slope in $f(v_\parallel)$ vs. $v_\parallel$ must be between the energy of electrons just arriving and that of the electrons whose flux is a maximum. As an estimate of this critical energy E_1, we use 1.5 times the energy of electrons just arriving at the time of commencement of the type III burst at 1 AU. We measure the electron flux $N(E_1)$ at that energy E_1.

For the radio waves we measure the value of the maximum flux density $S(2f_{pW})$ at $f \approx 2f_{pW}$, i.e., at the frequency twice the local plasma frequency. This frequency is relatively near f_{pW} (thereby preserving most of the correlation between the particles producing the radiation and those observed at the spacecraft), but far enough above it to be unaffected by the typical low frequency cutoff [*Leblanc et al.*, 1995].

The characteristics of the ten events are given in Table 1. As seen in the 4th column, there were four events where fast electrons were observed but no Langmuir waves; as the time of commencement in these cases we used an extrapolation of the radio start times to 1 AU, i.e., to $f = f_{pW}$. The parallel speeds of electrons producing the radio waves are given in the 5th column; they range from 0.09 to 0.19 c, within the range of previous measurements. The corresponding parallel energy ranges from 2.1 to 9.2 keV (6th column) while the critical energy E_1 estimated from the electron fluxes ranges from 4.5 to 17 keV (7th column). The average pitch angles from the Sun to 1 AU derived from these values range from 34° to 54° (8th column). The radio flux at $f \approx 2f_p$ ranges from $10^{4.1}$ to $10^{6.7}$ SFU (9th column), while $N(E_1)$, the electron flux at the critical energy E_1 ranges from 0.02 to 5.0 (cm^2 s ster eV)$^{-1}$.

The last two events in the table are noteworthy because their electron fluxes are exceptionally high. These two events originated from a very powerful active region, one that produced several intense flares and a giant magnetic cloud that is the subject of several studies. Event 10, October 20, 1995, was the strongest of the 10 events at radio wavelengths, and it produced intense electron fluxes at all energies that lasted for more than a day.

As mentioned, there were four events where intense fluxes of electrons were observed together with type III radio bursts descending nearly to the plasma frequency, but no Langmuir waves were recorded. The explanation of this anomaly deserves study. Possible reasons include the following: (1) The clumps of Langmuir waves of these events were sparse, and the solar wind was convected past the spacecraft without its encountering any clumps [e.g., *Reiner et al.*, 1992]. (2) Langmuir waves are generated only in the core of the electron stream, and in these cases the spacecraft was situated outside of that core.

Regarding the values of parallel speed, 0.09 to 0.19 c, derived from radio waves, we now consider the possibility that they are too low because the start times

of Langmuir waves are systematically delayed at the spacecraft relative to the start of Langmuir waves at the same f_p in other volumes permeated by the electron beam. Were this the case, then the start times of the type III would systematically lie ahead of the curve connecting the flare time to the Langmuir wave commencement time. In fact, only rarely do we find this to be true: in most events the Langmuir wave commencement lies within the uncertainty of the extrapolation of type III commencements to the local plasma frequency. Figure 5a is a good example where an extreme extrapolation gives a type III commencement at 25 kHz about 0.1 hour earlier than the Langmuir wave start; this would change $v_\parallel$ from 0.19 to 0.21 c. Further, as illustrated by the four events described in the preceding paragraph, the extrapolation of start times to the local f_p gives values of $v_\parallel$ within the range of the others.

Another possible reason that our values of $v_\parallel$ are too low is that we utilize an improper density scale when generating plots such as Figure 5a. We emphasize that the density-radial distance relation, the right-hand scale of Figure 5a, is not arbitrary: the most important parameter is f_{pW}, i.e., f_p at 1 AU, which is known. The other frequencies are scaled from that using $f_p(R) = f_{pW}\, R^{-\alpha}$, where we have assumed $\alpha = 1.0$. The value of the exponent α is not known precisely. High values of α have been suggested, e.g., $f_p \propto R^{-1.35}$ in the RAE model. These lead to an exceptionally high density in the corona, and are in conflict with more direct measurements. *Bougeret et al.* [1984], using Helios in situ measurements from 0.3 to 1 AU, derived $\alpha \approx 1.05$. For the middle-to-outer corona, the Saito model gives $\alpha \approx 1.07$ [e.g., *Saito et al.*, 1977].

We have generated Figure 5a using other values of α. When we put $\alpha = 1.35$, the extreme RAE value, the radial distances of high-frequency sources ($f \gtrsim 500$ kHz) are approximately 2.5 times higher. However, the extrapolated type III start time at 1 AU is moved forward by less than 0.1 hour because the radial distances of low frequency sources are only slightly larger. Thus the derived $v_\parallel$ is changed only from 0.19 to 0.21 c. With smaller, more reasonable values of α, the change from 0.19 c is negligible.

5. Theory

In this section we obtain theoretical expressions for the variation of the radio flux with the beam parameters using results from stochastic growth theory.

Stochastic growth theory implies that, to zeroth order, a type III electron beam propagates in a state of marginal stability on average. However, fast electrons tend to outrun slow ones, and this leads to an increase in the beam slope with time for a beam of finite duration. *Robinson* [1996] used the balance between beam build-up and quasilinear relaxation by stochastically growing Langmuir waves to show that the total power per unit volume that is stochastically transferred from beam electrons to Langmuir waves via the bump-on-tail instability is

$$P \approx \frac{2}{3x}\frac{v_\parallel}{\Delta v_\parallel}\left(\frac{1}{2}mv_\parallel^2\right)(N_b v_\parallel), \tag{1}$$

where m is the electron mass, $v_\parallel$ the velocity of the beam electrons parallel to the magnetic field, N_b the number density of beam electrons, $\Delta v_\parallel$ the spread of parallel beam velocities, and x is the distance the beam has propagated from the Sun. If we introduce the parallel electron flux $N(E_\parallel) = N_b v_\parallel$ and the parallel energy $E_\parallel = \frac{1}{2}mv_\parallel^2$, (1) becomes

$$P \approx \frac{2}{3x}\frac{v_\parallel}{\Delta v_\parallel}E_\parallel N(E_\parallel). \tag{2}$$

Beam-driven Langmuir waves L can undergo electrostatic decay into a product Langmuir wave L' and an ion-sound wave S via the process $L \rightarrow L' + S$. Extensive evidence has been found that it is this process that saturates the growth of Langmuir waves in interplanetary type III sources [*Cairns and Robinson*, 1995]. In the most commonly accepted model of type III emission, harmonic emission occurs via the coalescence of a product Langmuir wave L' with a beam-driven one L to yield an electromagnetic wave T near twice the plasma frequency: $L + L' \rightarrow T$ [*Melrose*, 1986]. Likewise, fundamental emission occurs via the decay of a beam-driven Langmuir wave into an electromagnetic wave T' and an ion-sound wave S': $L \rightarrow T' + S'$. *Robinson and Cairns* [1993] and *Robinson et al.* [1994] argued that this process has too high a threshold to proceed unless it is stimulated through the waves S' being produced by the electrostatic decay $L \rightarrow L' + S$; i.e., that S and S' should be identified with the same population of sound waves.

On the basis of the processes discussed in the previous paragraph, *Robinson and Cairns* [1993] showed that the volume emissivities for fundamental (F) and harmonic (H) radiation can be written as

$$j_M = \frac{\phi_M}{\Delta\Omega_M}P, \tag{3}$$

where $M = F$ or $M = H$, ϕ_M is the energy conversion efficiency from Langmuir waves to the mode in question, and $\Delta\Omega_M$ is the solid angle into which the waves M are radiated. By analyzing the dynamics of the relevant nonlinear processes in detail, they found

$$\phi_H \propto v_\parallel^2\frac{v_\parallel}{\Delta v_\parallel}\zeta_H, \tag{4}$$

$$\phi_F \propto \frac{\gamma_{L'}}{\gamma_S}\frac{v_\parallel}{\Delta v_\parallel}\zeta_F, \tag{5}$$

where all quantities not associated with the beam have been suppressed here, since we are only interested in beam-dependent variations. The quantities $\gamma_{L'}$, γ_S, ζ_F, and ζ_H are discussed in the next paragraphs.

The terms $\gamma_{L'}$ and γ_S in (3) are the absorption coefficients for the product waves in the electrostatic decay $L \rightarrow L' + S$ of a beam-driven Langmuir wave L

into another Langmuir wave L' and an ion-sound wave S. These coefficients appear because fundamental emission can only proceed under interplanetary type III conditions if it is stimulated by the sound waves S from electrostatic decay, as discussed above [*Robinson and Cairns,* 1993; *Robinson et al.,* 1994]. *Robinson et al.* [1994] showed that the efficiency of energy conversion to fundamental emission depended on the detailed dynamics and time evolution of the waves involved. Hence the damping rates of the waves L' and S affect the overall efficiency of the process because they affect the lifetimes of the waves involved. In terms of the beam velocity, standard expressions for these damping coefficients [*Melrose,* 1986] give

$$\gamma_S \propto v_\parallel^{-1}, \tag{6}$$

$$\gamma_{L'} \propto v_\parallel^{1-q}, \tag{7}$$

where the tail of the reduced (i.e., projected into one dimension) electron distribution function has been assumed to vary as v^{-q}. Observations imply $q \approx 4$ [*Scudder,* 1994].

Not all waves L, L', S, and S', present can participate in the above nonlinear processes for the generation of fundamental and harmonic emission. The weak-turbulence kinematic requirements of frequency matching and wave vector matching restrict the participating waves to a fraction ζ_M of the total present. This fraction can be expressed in terms of an integral that occurs in the nonlinear rate equation for the process in question [*Robinson and Cairns,* 1993; *Robinson et al.,* 1994] and has a maximum value of unity.

Detailed analysis by *Willes et al.* [1995, 1996] and *Willes and Robinson* [1997] showed that $\zeta_H \sim 1$ is a reasonable approximation under the relevant conditions in the interplanetary medium. Hence beam-dependence of this quantity can be neglected here.

The quantity ζ_F has never been accurately estimated, although *Robinson and Cairns* [1993] concluded that it was $\sim 2 \times 10^{-3}$ for three events they considered. Here we need only determine the scaling of ζ_F with beam parameters. This can be done by weighting the spectrum of ion-sound waves generated by the electrostatic decay $L \rightarrow L' + S$ by the strength of their coupling when participating in fundamental emission via the process $L \rightarrow T' + S$. In other words, we calculate the fraction of ion-sound waves produced by electrostatic decay that can also participate in electromagnetic decay to yield fundamental emission. This is done next.

We begin by noting that the spectrum of beam-generated Langmuir waves is centered near a parallel (relative to the beam direction) wave number $k_{L0} = \omega_p/v_\parallel$, with a fractional width of order $\Delta v_\parallel/v_\parallel$. Ignoring variations in the spectrum with perpendicular wave number for the present approximate purposes, we approximate this spectrum by the Gaussian

$$I_L(k_L) = \exp\left[-\frac{(k_L - k_{L0})^2}{\Delta k_L}\right], \tag{8}$$

with

$$\Delta k_L = \beta \frac{\omega_p}{v_\parallel}\frac{\Delta v_\parallel}{v_\parallel}, \tag{9}$$

where $\beta \approx 1/3$ is a constant that ensures the spectrum decreases substantially at $k_L = k_{L0}(1 \pm \Delta v_\parallel/2v_\parallel)$, which correspond to the maximum and minimum beam-driven wave numbers. The spectrum of ion-sound waves S can likewise be approximated by the Gaussian

$$I_S(k_S) = \exp\left[-\frac{(k_S - 2k_{L0} + k_0)^2}{(2\Delta k)^2}\right], \tag{10}$$

with

$$k_0 = \frac{2\omega_p}{3V}\sqrt{\frac{(1 + 3T_i/T_e)m}{M}}, \tag{11}$$

where M is the ion mass, V is the electron thermal velocity, and T_e and T_i are the electron and ion temperatures, respectively. The peak of this Gaussian is at $k_S = 2k_L - k_0$, where the rate of production of ion-sound waves by electrostatic decay peaks [*Melrose,* 1986].

The coupling of ion-sound waves at k_S to fundamental emission via $L \rightarrow T + S'$ is closely proportional to the value of the Langmuir spectrum at k_S, because of the need for wave vector (momentum) conservation and the smallness of the electromagnetic wave vector [*Robinson et al.,* 1994; *Robinson and Cairns,* 1993]. In other words, the requirement $k_L = k_S + k_{T'}$ implies $k_L \approx k_S$. Making this approximation, the overlap integral that determines the parameter ζ_F can then be written

$$\zeta_F = A \int dk_S I_S(k_S) I_L(k_S), \tag{12}$$

where A is a normalization coefficient that ensures $\zeta_F = 1$ for maximal overlap. This integral arises from the relevant term in the nonlinear rate equation, which involves the product of the Langmuir and ion-sound spectra, subject to kinematic constraints [*Melrose,* 1986; *Robinson et al.,* 1994]. After some algebra, (8), (10), and (12) yield

$$\zeta_F \approx \exp\left[-\frac{4(1 + 3T_i/T_e)m}{45\beta^2 M}\left(\frac{v_\parallel}{\Delta v_\parallel}\right)^2\left(\frac{v_c - v_\parallel}{V}\right)^2\right], \tag{13}$$

with

$$\frac{v_c}{V} = \frac{3}{2}\sqrt{\frac{M}{(1 + 3T_i/T_e)m}}. \tag{14}$$

Thus ζ_F increases rapidly with $v_\parallel$ until $v_\parallel = v_c$ before decreasing again.

We can now substitute the above results into (3) to find

$$j_H \propto \left(\frac{v_\parallel}{\Delta v_\parallel}\right)^2 E_\parallel^2 N(E_\parallel), \tag{15}$$

$$j_F \propto \left(\frac{v_\parallel}{\Delta v_\parallel}\right)^2 E_\parallel^{2-q/2} N(E_\parallel)\zeta_F, \tag{16}$$

where we have only retained factors that depend on the beam parameters.

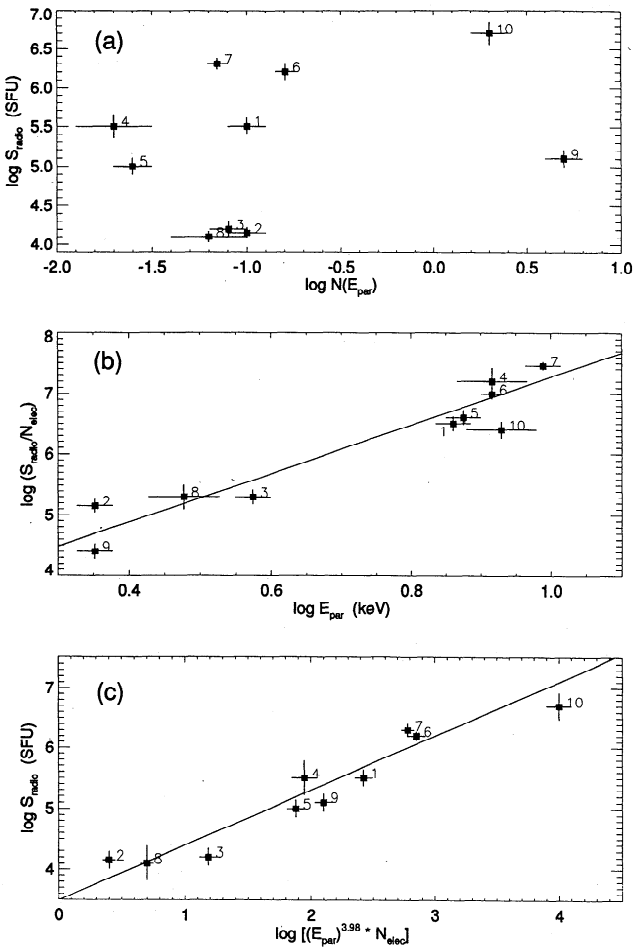

Figure 6. Comparison of radio flux densities with energies and fluxes of the type III-emitting electrons for 10 events. (a): Radio flux density vs. electron flux, showing essentially no correlation. The numbers refer to the entries in Table 1. Error bars (±1 sigma) are shown for both the abscissa and ordinate. (b): Radio flux density divided by electron flux vs. electron energy, with error bars for both coordinates. The best fit, least-squares line has a slope of 3.98; it shows a strong correlation ($r_c = 0.96$). (c): Similar to the top panel except that the abscissa is $E_{\|}^{3.98} N(E_{\|})$. The best fit, least-squares line is shown.

Before concluding this section, it is worth stressing that the above theory makes some important simplifying approximations, that can only be relaxed by a far more sophisticated analysis: (1) k_L and k_S have been assumed to significantly exceed k_0, (2) the value of β is only approximate, (3) the spectra are assumed approximately Gaussian, and (4) there is assumed to be no systematic variation of $\Delta v_{\|}/v_{\|}$ with $v_{\|}$.

6. Interpretation

We use the data of Table 1 to determine whether there is a direct proportionality between the electron flux $N(E_{\|})$ and the radio flux density $S(2f_{pW})$. Figure 6a shows that there is no perceptible correlation. However, (15) and (16) demonstrate that the energy $E_{\|}$ is important to the emission process, as well as the electron flux $N(E_{\|})$.

Therefore we compare the observations with (15) and (16) assuming that the radio flux $S(2f_{pW})$ at the spacecraft is proportional to the volume emissivity at the source. We also assume that the total electron flux $N(E_1)$ measured by the spacecraft is proportional to $N(E_{\|})$ in the theory. Statistically, this is a reasonable assumption since the typical pitch angles of the beam electrons ($\langle \alpha_e \rangle \approx 46°$) do not vary dramatically from event to event; it could of course be improved in a more detailed analysis.

We now consider whether the peak radio flux is due to fundamental or to harmonic emission.

First, to test the hypothesis that the peak flux is due to harmonic emission, we plot $S(2f_{pW})/N(E_{\|})$ vs. $E_{\|}$ on a log-log scale. Here the correlation is excellent. The correlation coefficient is $r_c \approx 0.96$, and the slope of the weighted best fit line is 3.98 ± 0.15. This slope is too high to be consistent with the value of 2 expected from (15) for harmonic emission if $\Delta v_{\|}/v_{\|}$ is independent of $v_{\|}$.

To show this result in a different way, we now use the exponent 3.98, and on Figure 6c we plot $S(2f_{pW})$ vs. $E_{\|}^{3.98} N(E_{\|})$. The correlation is the same, with the best-fit straight line given by

$$\log_{10}[S(2f_{pW})] = 3.49 + 0.90 \log_{10}[E_{\|}^{3.98} N(E_{\|})]. \quad (17)$$

Next, the hypothesis that the peak radio flux is due to fundamental emission can be tested (for $q \approx 4$ in (16)) by plotting $S(2f_{pW})/N(E_{\|})$, not vs. $E_{\|}$ as above, but vs. $(v_c - v_{\|})^2/V^2$ on a log-linear scale (see (13)). To do this we assume typical parameters of $V \approx 1.8 \times 10^6$ m s^{-1} and $T_i = 0.2T_e$ at the source, giving $v_c \approx 51V$. The results, shown as squares in Figure 7, exhibit a linear correlation coefficient of approximately 0.9. The slope of the line of best fit is $-(2.4 \pm 0.5) \times 10^{-3}$, which compares well with the value of $-3.4 \times 10^{-5} (v_{\|}/\beta \Delta v_{\|})^2$ predicted from (16) using $\beta = 1/3$, provided $\Delta v_{\|}/v_{\|} \approx 0.3 - 0.4$. This range of full beam widths agrees well with observations [*Cairns and Robinson*, 1995] and strengthens our confidence in the approximations made in Section 5. We thus conclude that the peak flux is consistent with fundamental emission, but not harmonic.

The results in Figure 7 allow us to use (13) to estimate the value of ζ_F, noting that $\zeta_F = 1$ at $v_{\|} = v_c$. We find $2.5 \times 10^{-4} \lesssim \zeta_F \lesssim 0.3$ for the 10 events in Table 1, while the minimum value of ζ_F for slow beams is predicted to be of order 10^{-6}. These values neatly bracket the values of $(2 - 2.5) \times 10^{-3}$ inferred by *Robinson and Cairns* [1993] for radiation at $2\omega_p$ in three events observed by ISEE 3 at 1 AU (see their paper for details). Using their beam and plasma parameters, including individual values of T_e and T_i for the three events (extrapolated to the source), we have plotted their events in Figure 7 using triangular symbols. These points are quite consistent with the 10 of the present study, despite the very dif-

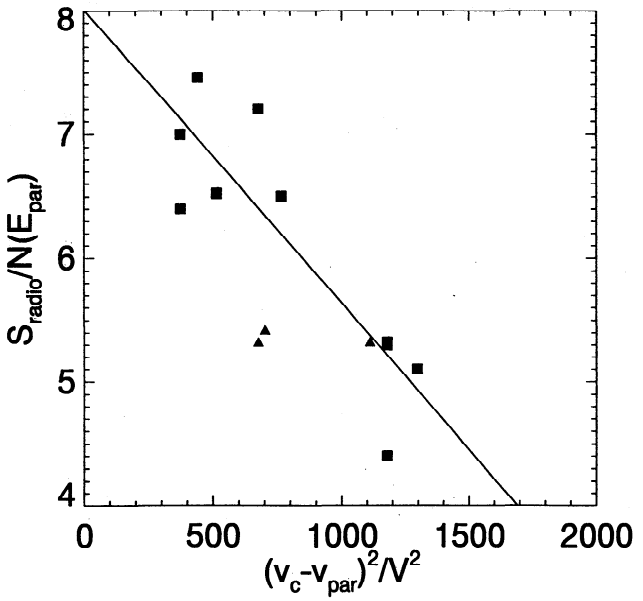

Figure 7. Plot of $S(2f_{pW})/N(E_{\|})$ vs. $(v_c - v_{\|})^2/V^2$ for the 10 events in Table 1 (squares) and three events discussed by *Robinson and Cairns* [1993] (triangles). The line of best fit to the squares is shown.

ferent way of inferring their vertical positioning on the plot.

Taken at face value, the results in Figure 7 imply that there is only moderate reabsorption of the peak emission within the source. The reason for this is that *Robinson and Cairns*'s [1993] results did not correct for such reabsorption, which would tend to reduce the apparent value of ζ_F from its intrinsic value. *Robinson and Cairns*'s [1993] three points do all lie below the line of best fit, but only by a factor of ~ 4 on average. To the extent that these events are typical, this implies that $\sim 25\%$ of the peak emission escapes the source. It should be noted, however, that the events analyzed by *Robinson and Cairns* [1993] were actually particularly intense, implying that they should almost certainly lie above the line in Figure 7. This would imply that a much smaller fraction of the peak emission can escape the source. Work is currently in progress to resolve this point [*Robinson and Cairns*, 1997].

A final point to be noted, by comparison with *Robinson and Cairns*'s [1993] work, is that their inferred efficiencies of emission at f_{pW} were roughly an order of magnitude lower than at $2f_{pW}$, despite $v_{\|}/V$ being higher. This supports *Leblanc et al.*'s [1995] conclusion that there is a cutoff in type III activity near 20 kHz, i.e., at 1 to 1.5 AU.

7. Conclusions

Observations of ten type III bursts that were associated with electron beams have demonstrated how the radio flux density depends on the electron flux and the critical energy, i.e., the energy where the two-stream instability occurs, where there is a positive slope in the reduced distribution function. That critical energy is heavily weighted in the empirical relationship $S_{\rm radio} \propto E_{\|}^{\beta} \times N(E_{\|})$, with $\beta \approx 4$.

Recent observations of interplanetary type III bursts that intersect the spacecraft (i.e., where fast electrons and/or Langmuir waves are recorded) have provided evidence that the radiation from onset until approximately the peak is at the fundamental. Near and after the peak, the mode of emission is unknown. For bursts that do not intersect the spacecraft, there is no direct means of determining the mode of emission.

The evidence is very strong that the initial radiation is at the fundamental for almost all bursts accompanied by fast electrons and/or Langmuir waves, i.e., for 58 of the 61 bursts reported in the works of *Kellogg* [1980], *Dulk et al.* [1984], *Dulk et al.* [1987], and *Hoang et al.* [1994]. This evidence includes the following: (1) Usually the trace of burst start times leads closely to the start of Langmuir waves, and for the few bursts studied, to the first appearance of a positive or marginally positive slope on the reduced electron distribution. To attribute this initial radiation to the harmonic is to propose that the effect precedes the cause, i.e., that harmonic radiation is emitted before the electron distribution is unstable at the appropriate f_p. (2) In very rare cases (2 of 61) the trace of burst start times indicates that the dominant mode changed from fundamental to harmonic midway from the Sun [*Hoang et al.*, 1994], and in one case from harmonic to fundamental [*Kellogg*, 1980]. These rare cases illustrate that the method of tracing start times can distinguish fundamental from harmonic radiation. (3) For the event reported in detail here, the more intense radiation at decametric wavelengths is known to be fundamental from its polarization properties, and the burst development is continuous to kilometer wavelengths. (4) In general, fundamental radiation at kilometer wavelengths is distinguished from harmonic by its faster rise times, smaller source sizes, higher brightness temperatures in excess of 10^{14} K, and a more pronounced east-west asymmetry of brightness temperature resulting from higher directivity [*Dulk et al.*, 1984]. (5) From theory, the high brightness temperatures of interplanetary type III bursts are compatible with fundamental but not harmonic radiation [*Melrose*, 1989].

Finally, the theoretical analysis of this paper shows that the dependence of the emissivity at burst peak on the beam properties is consistent with fundamental emission but not with harmonic emission. Both the functional form and numerical value of the slope of the fit in Figure 7 are consistent with theory for beam parameters in the observed range. These results are consistent with those of *Robinson and Cairns* [1993], and have allowed us to infer values for the energy conversion efficiency from beam kinetic energy to fundamental emission, estimating the parameter ζ_F in a new way.

Acknowledgments. We thank C. Meetre of NASA (GSFC) for developing the software used to analyze WAVES observations, P. Zarka and L. Denis for assistance in obtaining the spectrum from the decametric array at Nançay, and

I. H. Cairns for helpful discussions. The WAVES experiment is a joint project of the Observatoire de Paris, NASA/GSFC, CETP and the University of Minnesota. The 3-D Plasma and Energetic Particles investigation at the University of California is supported in part by NASA grant NAG5-2815. Additional support has come from the Centre National de la Recherche Scientifique, the Australian Research Council, and the Australian Academy of Science.

The Editor thanks M. Reiner and another referee for their assistance in evaluating this paper.

References

Boischot, A., et al., A new high gain, broadband, steerable array to study Jovian decametric emission, *Icarus, 43,* 399, 1980.

Bougeret, J.-L., J.H. King, and R. Schwenn, Solar radio bursts and in-situ determination of electron density, *Sol. Phys. 90,* 401, 1984.

Bougeret, J.-L., et al., Waves: The radio and plasma wave investigation on the Wind spacecraft, *Space Sci. Rev., 71,* 231–263, 1995.

Cairns, I. H., and P.A. Robinson, Ion acoustic wave frequencies and onset times during solar type III radio burts, *Astrophys. J., 453,* 959, 1995.

Dulk, G.A., and S. Suzuki, The positions and polarization of type III solar bursts, *Astron. Astrophys. 88,* 203, 1980.

Dulk, G.A., J.-L. Steinberg, and S. Hoang, Type III bursts in interplanetary space - Fundamental or harmonic?, *Astron. Astrophys. 141,* 30, 1984.

Dulk, G.A., J.-L. Steinberg, S. Hoang, and M.V. Goldman, The speeds of electrons that excite solar radio bursts of type III, *Astron. Astrophys. 173,* 366, 1987.

Ergun, R.E., et al., Wind spacecraft observations of solar impulsive electron events associated with solar type III radio bursts, *Astrophys. J.,* in press, 1997.

Ginzburg, V.L., and V.V. Zheleznyakov, On the possible mechanisms of sporadic solar radio emission, *Sov. Astron. AJ, 2,* 653, 1958.

Gurnett, D.A., and R.R. Anderson, Electron plasma oscillations associated with type III radio bursts, *Science, 194,* 1159, 1976.

Hoang, S., G.A. Dulk, and Y. Leblanc, Interplanetary type III radio bursts that approach the plasma frequency: Ulysses observations, *Astron. Astrophys. 289,* 957, 1994.

Kellogg, P.J., Fundamental emission in three type III radio bursts, *Astrophys. J., 236,* 696, 1980.

Leblanc, Y., G.A. Dulk, and S. Hoang, The low radio frequency limit of solar type III bursts: Ulysses observations in and out of the ecliptic, *Geophys. Res. Lett., 22,* 3429, 1995.

Lin, R.P., Observations of the 3D distribution of thermal to near- relativistic electrons in the interplanetary medium by the Wind spacecraft, in *Coronal Physics From Radio and Space Observations,* edited by G. Trottet, pp. 93-107, Springer-Verlag, New York, 1997.

Lin, R.P., D.W. Potter, D.A. Gurnett, and F.L. Scarf, Energetic electrons and plasma waves associated with a solar type III radio burst, *Astrophys. J., 251,* 364, 1981.

Lin, R.P., et al., A three-dimensional plasma and energetic particle investigation for the Wind spacecraft, *Space Sci. Rev., 71,* 125, 1995.

Lin, R.P., et al., Observation of an impulsive solar electron event extending down to 0.5 keV energy, *Geophys. Res. Lett., 23,* 1211, 1996.

Melrose, D.B., *Instabilities in Space and Laboratory Plasmas,* Cambridge Univ. Press, New York, 1986.

Melrose, D.B., The brightness temperature of solar type III bursts, *Sol. Phys. 120,* 379, 1989.

Reiner, M.J., J. Fainberg, and R.G. Stone, Detection of fundamental and harmonic type III radio emission and the associated Langmuir waves at the source region, *Astrophys. J., 394,* 349, 1992..

Robinson, P.A., Clumpy Langmuir waves in type III radio sources, *Sol. Phys. 139,* 147, 1992.

Robinson, P.A., Stochastic wave growth, power balance and beam evolution in type III solar radio sources, *Sol. Phys. 168,* 357, 1996.

Robinson, P.A., and I.H. Cairns, Stochastic growth theory of type III solar radio emission, *Astrophys. J., 418,* 506, 1993.

Robinson, P.A., and I.H. Cairns, Fundamental and harmonic emission in type III solar radio bursts, *Sol. Phys. 154,* 335, 1994.

Robinson, P.A., and I.H. Cairns, Fundamental and harmonic emission in type III solar radio bursts. I. Emission at a single location or frequency. II. Dominant modes and dynamic spectra, *Sol. Phys.* in press, 1997.

Robinson, P.A., I.H. Cairns and D.A. Gurnett, Connection between ambiant density fluctuations and clumpy Langmuir waves in type III radio sources, *Astrophys. J., 387,* L101, 1992.

Robinson, P.A., I.H. Cairns, and D.A. Gurnett, Clumpy Langmuir waves in type III radio sources - Comparison of stochastic growth theory with observations, *Astrophys. J., 407,* 790, 1993a.

Robinson, P.A., A.J. Willes, and I.H.Cairns, Dynamics of Langmuir growth-rate fluctuations in type III solar radio sources, *Astrophys. J., 408,* 720, 1993b.

Robinson, P.A., I.H. Cairns, and A.J. Willes, Dynamics and efficiency of type III solar radio emission, *Astrophys. J., 422,* 870, 1994.

Saitô, K., A.I. Poland, and R.H. Munro, A study of the background corona near solar minimum, *Sol. Phys.* 55, *121,* 1977.

Scudder, J., Ions and electron suprathermal tail strengths in the transition region: support for the velocity filtration model of the corona, *Astrophys. J., 427,* 446, 1994.

Steinberg, J.-L., G.A. Dulk, S. Hoang, A. Lecacheux, and M.G. Aubier, Type III radio bursts in interplanetary medium - The role of propagation, *Astron. Astrophys. 140,* 39, 1984.

Willes, A. J., and P.A. Robinson, Improved predictions of electric field strengths and volume emissivities in second harmonic type III solar radio emission, *Sol. Phys. 171,* 393, 1997.

Willes, A. J., P.A. Robinson, and D.B. Melrose, Solar second harmonic plasma emission and the head-on approximation, *Publ. Astron. Soc. Australia, 12,* 197, 1995.

Willes, A. J., P.A. Robinson, and D.B. Melrose, Second harmonic electromagnetic emission via Langmuir wave coalescence, *Phys. Plasmas, 3,* 149, 1996.

J.-L. Bougeret, G.A. Dulk and Y. Leblanc, DESPA, Observatoire de Paris, 92195 Meudon, France. (e-mail: dulk@obspm.fr; leblanc@obspm.fr; bougeret@obspm.fr)

P.A. Robinson, Dept. of Theoretical Physics, University of Sydney, Sydney, NSW 2006, Australia. (e-mail: robinson@phys.usyd.edu.au)

R.P. Lin, Space Sciences Laboratory, University of California, Berkeley, CA 94720. (e-mail: rlin@sunspot.ssl.berkeley.edu)

(Received March 13, 1997; revised September 30, 1997; accepted October 21, 1997.)